EM FIELD DISTRIBUTION AMD PROPAGATION IN SOME REALISTIC SCENARIOS

D. Kakulia, L. Manukyan, D. Mazmanov, A. Razmadze, R. Zaridze

Tbilisi State University, Tbilisi, 0128, Georgia,

email: lae@laetsu.org

Abstract

This is an overview article related to methodology of evaluating the exposure to EM energy in various realistic scenarios and for better understanding of the field EM distributions in the outdoor and indoor environments nearby powerful EM sources or base stations [1]. Several scenarios are considered. First, is a closed or semi-open objects that are analyzed as a resonators with some Q-factor for which a numerical EMC study related to the resonant enhancement of the EM fields within the volume is described with the particular example of in-vehicles scenario. Second is the studying outdoor field propagation nearby and around some obstacles and evaluation of the field distribution in this case. The list topic is related to investigation of human exposure to EM fields in a wide frequencies range. All the simulated scenarios are reasonably realistic and include many practical exposure and propagation conditions.

1. INTRODUCTION

During last years the rapid growth of number of the cellular base stations (BS), and different type of antennas, which transmit high-powered electromagnetic (EM) signals were observed. Today, health effects related to EM exposure are one of the most common research areas in area of EM Compatibility. Besides EM field interaction with human body, the much wider area of research is related to EM interaction between sensitive electronics equipment including those in cars, hospitals, etc., that in turn can lead in certain instances to catastrophic malfunctioning of the devices. Special international committees have been organized to establish allowable limits and health safety standards related to EM maximum permissible exposure

levels as well as background level of EM energy. According to recommendations of the scientists involved in this area, most acceptable would be the uniform distribution of the energy radiated from the base stations. The recommendations are also intended to not compromise the realization of stable wireless communication and at the same time to reduce the potential health risk by ensuring adherence to international safety standards. Description of a character of EM field propagation in the wide frequency range of practical applications in various conditions including urban scenarios computer modeling with simplified scenarios is usually applied.

2. APPROACH

As The Method of Auxiliary Sources (MAS) [2, 6] as a mathematical tool for solving current EM problem has been applied in the example described in this paper. In the diffraction problems involving cavities with apertures MAS may be efficiently utilized. As it usually deals with continues boundaries it was proposed to apply MAS to the incomplete surface of cavities which is completed by the imaginary surface covering the apertures. One such continue boundary surface has been constructed the whole areas is divided into ineer and outer domain and a two auxiliary surfaces can be introduced on both domain as it usually the case in using MAS for solid homogeneous objects. Therefore, the two sets of Auxiliary Sources (AS) are placed on the auxiliary surfaces, l in inside and lout outside as shown in Figure 1a. The inner AS on surface l in represent the field outside of the cavity and on the boundary l, while the outer AS located on surface l out represent the field inside the cavity.

The Boundary condition for the perfectly conducting surface is used on the both inside and outside surface of the cavity. Thus the tangential components of the total electric field is enforced to be must be zero.

$$\left[\sum_{n=1}^{N} j_n \vec{E}(\vec{r}-\vec{r}_n) - \vec{E}^{inc}(\vec{r})\right]\Bigg|_{\tau} = 0 \qquad (1)$$

where $\vec{r}_n$ - is the radius vector of the n-th source, $\vec{r}$ is the radius vector of the point of observation $\vec{r} \in l$. On the imaginary surface the continuity of the total tangential magnetic and electric fields is enforced.

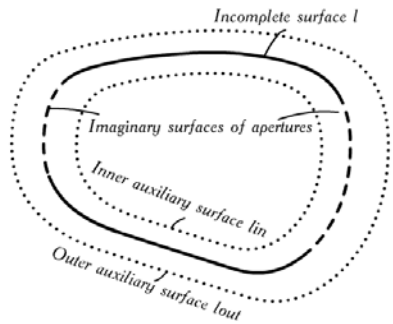

Figure 1a. MAS model of cavity with using auxiliary and imaginary surfaces

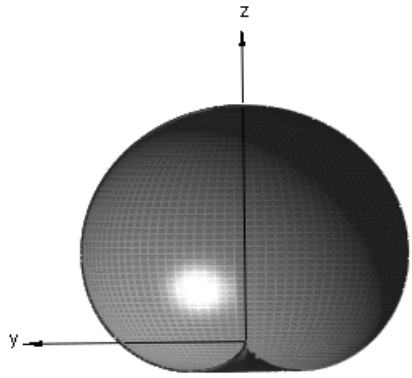

Figure 1b. Pattern of Combined Dipole

Those boundary conditions on the cavity surface and on the imaginary aperture surfaces lead to the set of equations which is very similar to the case of solving the scattering problem on dielectric object using MAS. In the latter case including the incident field the system of equations is as follows:

$$\begin{cases} \left[\sum_{n=1}^{N} j_n^{out}\vec{E}\left(k\sqrt{\varepsilon_{in}\mu_{in}}\left|\vec{r}_n-\vec{r}\right|\right)-\sum_{n=1}^{N} j_n^{in}\vec{E}\left(k\sqrt{\varepsilon_{out}\mu_{out}}\left|\vec{r}_n-\vec{r}\right|\right)\right]\Bigg|_{\tau} = \vec{E}^{inc}(\vec{r})\Big|_{\tau} \\ \left[\sum_{n=1}^{N} j_n^{out}\vec{H}\left(k\sqrt{\varepsilon_{in}\mu_{in}}\left|\vec{r}_n-\vec{r}\right|\right)-\sum_{n=1}^{N} j_n^{in}\vec{H}\left(k\sqrt{\varepsilon_{out}\mu_{out}}\left|\vec{r}_n-\vec{r}\right|\right)\right]\Bigg|_{\tau} = \vec{H}^{inc}(\vec{r})\Big|_{\tau} \end{cases} \quad (2)$$

where j_n^{out} and j_n^{in} are the coefficients of the auxiliary sources placed outside and inside the dielectric scatterer respectively; $\vec{E}^{inc}(\vec{r})$ and $\vec{H}^{inc}(\vec{r})$ are incident fields on the boundary surface; ε_{in}, μ_{in} and ε_{out}, μ_{out} are permittivity and permeability of inner and outer media. $\vec{E}(\vec{r})$ and $\vec{H}(\vec{r})$- E and H-field's functions of the auxiliary sources.

The requirement to satisfy the boundary conditions leads to the system of linear equations with unknown coefficients j_n, which have the physical meaning of the amplitude of the AS (dipole currents representing the AS in this particular case). The shape of an imaginary surface cannot be set arbitrarily, as it influences the efficiency

of the method. Usually one should avoid sharp corners on the boundaries when applying MAS. It is advisable to select a larger curvature radius of the boundary surface, since it allows coverage of a larger section of the boundary surface with only a few AS (therefore reducing the number of unknowns). In practice, finding an appropriate rounded surface does not pose difficulties. According to the MAS algorithm, the accuracy of the modeling is determined by: a) choosing the correct functions – Auxiliary Sources in order to represent the scattered field and b) correct distribution of AS on the auxiliary surfaces and determining the coefficients to satisfy the boundary conditions (to provide best fulfillment of boundary conditions in the least square sense).

The chosen base function (AS) satisfies the wave equation by itself. In our case we utilized the combined sources AS [3, 4]. The main distinction of this type of AS is a directionality of its pattern. The Figure 1b shows an example of such AS with a directional radiation pattern in a shape of cardioid of revolution. This, so-called Huygens' element [5] illuminates in one direction. Since the AS and their linear combination satisfies the wave equation and the geometry is the error of the solution can be determined by evaluating how accurately one satisfies the boundary conditions, which could be controlled easily. Another advantage of MAS is its ability to easily calculate currents induced on both the inner and outer surfaces of the boundary, which leads to the physical current flowing on each surface of the cavity in this example.

3. NUMERICAL RESULTS

3.1. Field distribution in some scenarios.

In this part we present some numerical results related to the behavior of resonance characteristics of open metallic objects with a cavity.

In the first scenario we apply the described above algorithm to the EMC problem of the vehicle with specific lossy dielectric body inside representing the driver model. The source of the electromagnetic wave, which produces initial, incident field, may be some internal antenna, the electronic devices or some external electromagnetic source.

As an example of geometry we consider four different cases using a simplified model of a car body: 1. the empty car body with front and back windows; 2. the same

car model but with the addition of wheel wells; 3. the first geometry with partition, similar to the engine firewall; 4. the empty car body with the addition of lossy dielectric body inside, to simulate presence of the driver. The dimensions of the car model are 5.0 x 2.5 x 1.5 m^3. Below we consider the case when the source of the EM field is a dipole located outside the car. The calculated resonance characteristics – integrated radar cross section (IRCS) – of the objects under investigation were obtained in a wide frequency range from 20 MHz to 640 MHz ands for all considered cases are presented in Fig.2.a).

As a general rule for of the IRCS, it must be proportional to $(ka)^2$. (where $k = 2\pi / \lambda$, a - is half of the biggest dimension of the car. $2a=5m$.) This fact alone already demonstrates the adequacy of the calculation results. Besides, there are the high values of radiated field observed at some frequencies that correspond to the resonances of the car cavities. Calculations of the near field show that in case of out of the resonance frequency field inside the car is very low. But at the resonances it becomes high. The first resonance appears at ka=5.31, which corresponds to 118 MHz (See Figure 2b).

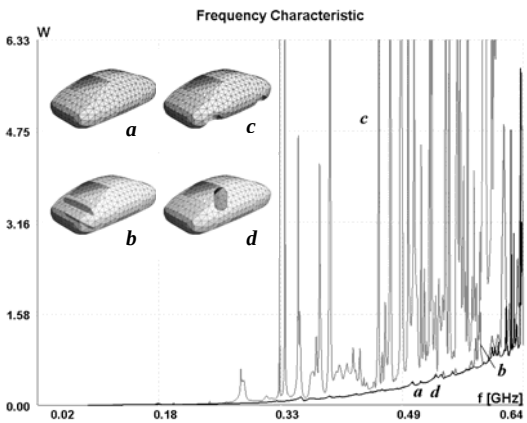

Figure 2a. Resonance curves for different geometry type in a wide range

More detailed investigations for some particular cases have been performed allowing tracking the process of eigen field formation inside the cavity. This methodology allows determining the basic characteristics of the cavity – eigen field (Figure3), eigen mode and eigen value.

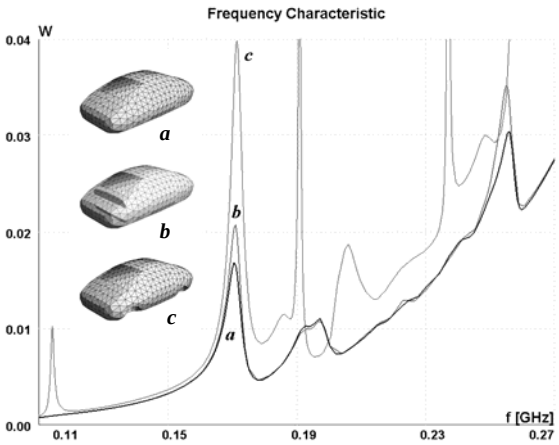

Figure 2b. Resonance curves for different geometry type near the first resonance

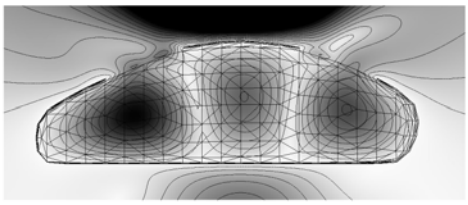

Figure 3. Resonance field distribution

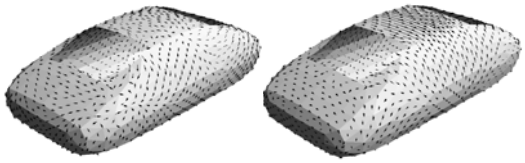

Figure 4.The induced inner (left) and outer (right) currents

In Figure 4 the induced current distribution on the metallic surfaces of the car at the resonant frequency of 174 MHz is shown. The detail investigations have shown that the current distribution inside the cavity has a standing wave nature while that on the outer surface is similar to a traveling wave. At the same time, strength of the electric field in some points inside the cavity could be much higher then outside in the traveling wave. These phenomenon arises especially at higher order resonances and are related to higher Q-factor.

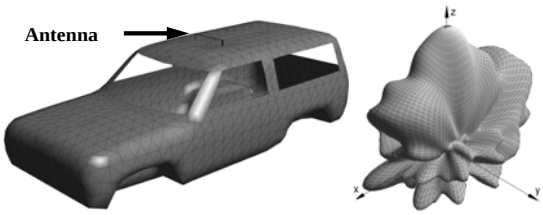

a) *b)*

Figure 5. a) The car model with wire antenna on head and b) Radiation pattern. Ka = 20

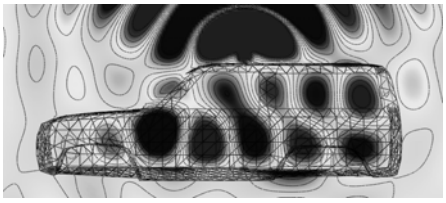

Figure 6. Field distribution in XOZ slice. Ka = 20. Antenna located on the roof

Next we considered the case when antenna (wire) is placed on the roof of the car (in our example – "Jeep" model is shown in Figure 5a.

Then the behavior of the field distribution inside the car is close to eigen field. The radiation pattern and the field distribution are presented in Figure 5b and Figure 6 correspondingly. The resonance in this picture corresponds to *ka*=20.

Another example below demonstrates an indoor field distribution. Rooms have resonant properties which might increase in special circumstances the EM field values several times inside the buildings. Room resonance properties are defined by room size, placement and size of the windows, doors and other objects in the room. Four different cases of room models with dimensions 3,5x4,5x3,0 m have been considered: a) closed room, b) room with one window, c) room with two windows, d) room with two windows and door. They are presented on Fig.7. A plane wave was with Z polarization has been chosen as an external source. The dimensions of windows and door are correspondingly: 1,26x0,7m and 1,57x0,9m. The number of unknowns is 1400.

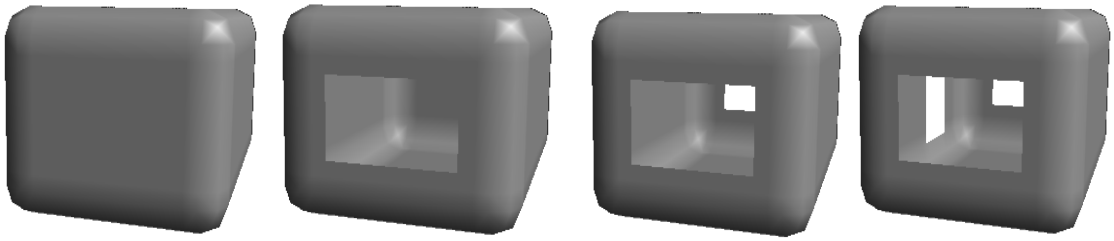

a) b) c) d)

Figure 7. Models of the rooms

Near field distribution at resonance frequency is presented in Figure 8. In case a) the field distribution on perfect conducting structure at the resonance frequency of 630 MHz is presented. As it is shown in the figure, wave does not reach the backside of structure. In case b) inside the room at the approximately same resonance frequency of 635 MHz a standing wave appears. The higher field values appear near the window, which is facing the incident wave source. In case c) at the same frequency the picture is approximately the same. The only difference is that amplitude of standing wave is decreased and its peak is slightly shifted. The larger decrease in case d) is observed. The location of resonant peaks changes slightly by adding other window openings in the room. At the same time, as it could be predicted from theory, the addition of window openings decreases the Q-factor of this structure. This is obviously related to more energy leakage through larger openings, therefore a buildup of the reactive field inside the room is less intensive.

Although the modeling of this problem was based on room models with PEC walls, the limited accuracy of fulfilling the boundary conditions may be interpreted as wall's ability to admit EM waves (the higher is residual the bigger is coefficient of admittance), that can represent the properties of concrete blocks with steel reinforcements.

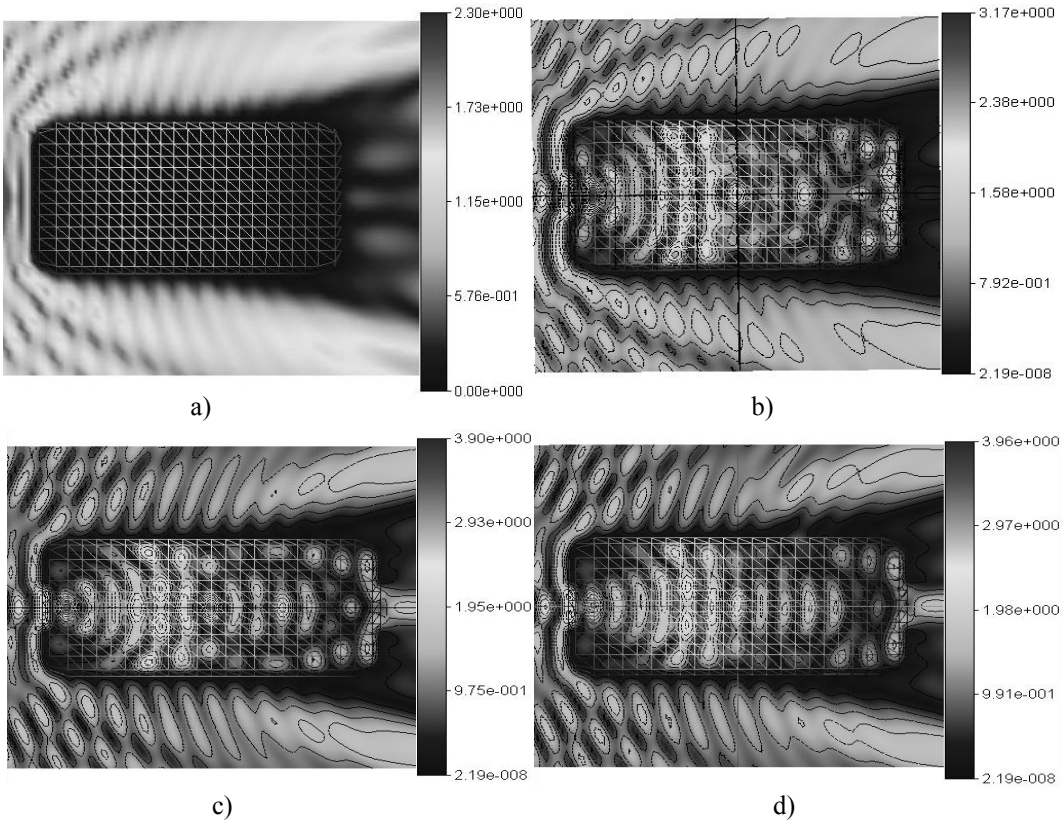

Figure 8. Field distribution. a) closed room; b)room with one window; c)room with two windows; d)room with two windows and door

3.2. Human Exposure

If the interests are in investigation of complex problem: Assessment of Average Human Exposure to RF Energy in Some Realistic Scenarios –then we need to know the EM field distribution, SAR, total absorbed EM energy and temperature rise inside the human for several realistic scenarios. For human model was chosen a homogeneous human “mummy” model with dimensions 1.75m, 0.45m and 0.3m. The model has permittivity and conductivity, which correspond to the average of human tissues.

Most actual scenario is the case when human model is located in the room. Now the main accent of researches was placed on human. Field distribution for frequency 500MHz is shown on Figure 9.

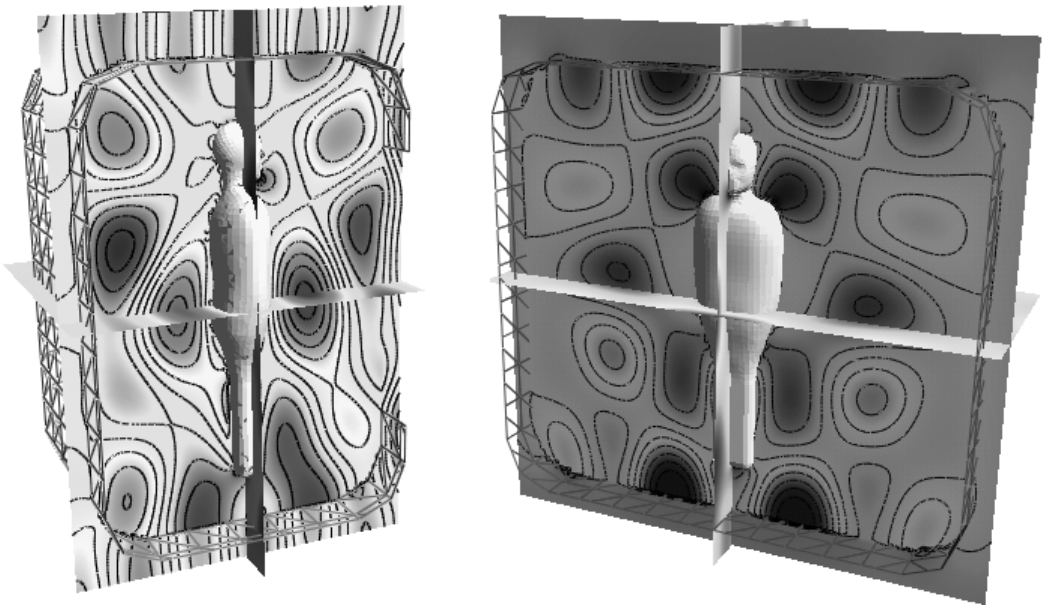

Figure 9. Field distribution in the room with human model inside. Room dimensions: 2.4 x 2.2 x 1.5 m^3, window: 1.10x1.25 m^2

Standing-wave factor determines peak and average values of power densities. Very high difference of the power density distribution and its variation takes place inside the rooms. SAR and power density distributions inside the human model should eventually be consider within this scenario. Below (See Figure 10) the comparison of SAR is presented. A left picture illustrates SAR distribution in "mummy" placed in free space (vacuum), and the right one – in the room model.

As it can be noticed from presented pictures, SAR value increases by placing mummy to the room, just as field's peak amplitude in the room is higher than in case without room. Temperature rise has the same character (Figure 11).

Next following results are dedicated to several outdoors scenarios. In the case of fixed geometry of the mountain, two different locations of the excitation (CBS) are considered: When CBS is far away and incident wave near the mountain could be considered as a plain wave (Figure 12a).

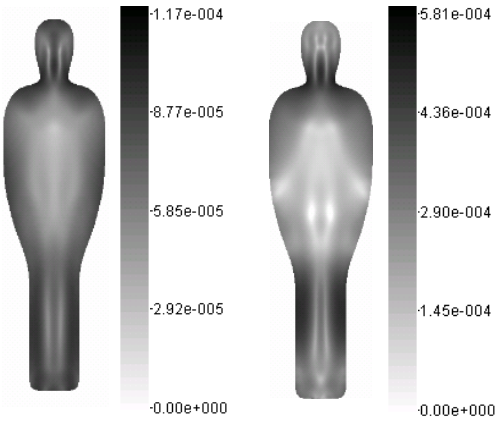

Figure 10. SAR Comparison for human model
In free space (left). In the room (right)

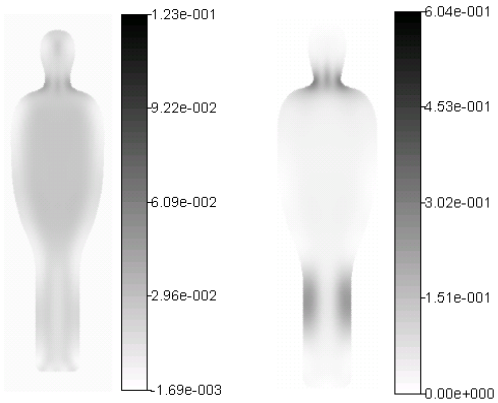

Figure 11. Temperature rise comparison for human model. In free space (left). In the room(right)

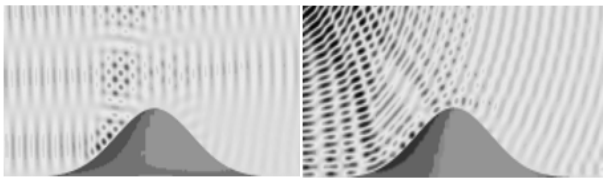

a) *b)*

Figure 12. a),b) Field distribution near the mountain for different source location

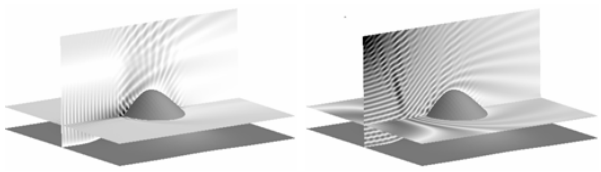

c) *d)*

Figure 12. c), d) Average power density distributions near the hill in 3D

The reflected wave is traveling up from the left side of the mountain and on the field pattern one streak has an upward direction getting the interference pattern. There are perpendicular traveling waves. During the investigation analogous phenomena takes place for lower frequencies. Based on these results, it should be assumed, that the same process can be observed at higher frequencies. Figure 12b shows the case when CBS is located close to the mountain and incident field is almost spherical wave. There are standing waves pattern appearing in front of the hill with higher peaks and average power densities relative to the first one. In Figure 12c and d, the power density distributions near the hill in several cross sections in 3D are presented, which corresponded cases of Figure 12a and b. At some elevation from the ground, there is difference: in case of CBS located far from the mountain the power, density distribution is practically uniform, unlike the situation in Figure 12d, where the areas of very low power exist.

The following case is a wall located in YZ plane (See Figure 13) and the source of incident field is an elementary dipole with Z polarization located in XZ plane. The wall has a square form and is placed on PEC ground. Field distributions are presented in Figure 13. In case a) the source position is not far from the wall. In case b) the source is placed far away. In both cases near the wall standing waves appear, while other side is in deep shadow.

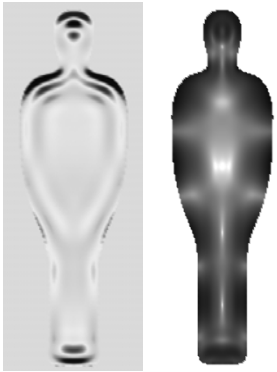

e) *f)*

Figure 12. e), f) E field and peak SAR distribution on human model, standing on the Ground near the hill correspondingly

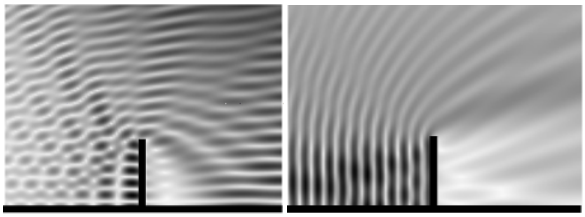

Figure 13. Field distribution in XOZ slices near the wall for different source positions (field values are normalized to the incident field level)

The frequency of the incident EM field is 0.9 GHz. For comparison below (See Figure 14) field distribution for two different cases is presented: 1) the model of human is exposed to the traveling wave and no other objects are nearby. 2) the model is exposed to the standing wave near the vertical obstacle from the example presented above. It should be mentioned that in both cases the higher value of the EM field is found mainly on the human surface.

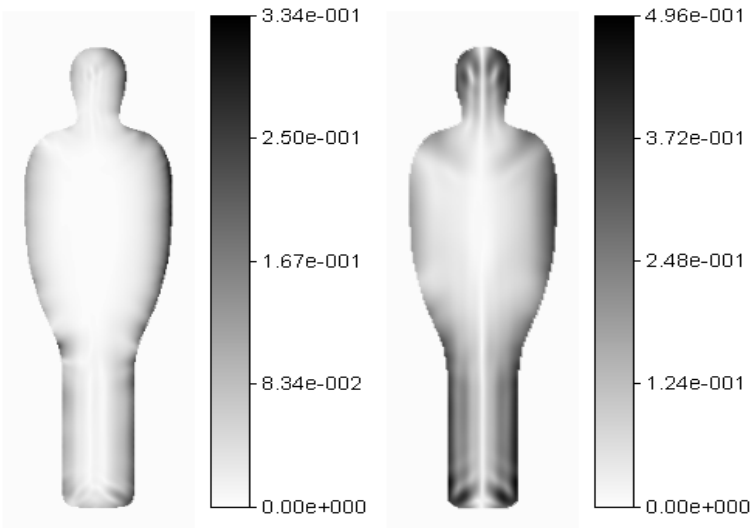

a) *b)*

Figure 14. Field distribution pattern inside the homogeneous body a) traveling and b) standing waves at frequency = 0.9GHz, Body parameters:
$\varepsilon_r = 55$, $\sigma = 1.35$

This is due to the relatively high conductivity of the tissues, which prevents penetration of the field inside the body. Wavelength inside the body is many times less than in free space. Besides, in this standing wave condition the field strength is higher than in traveling wave case. It means that exposure in the presented standing wave scenario is higher than in traveling wave example.

4. CONCLUSION

The motivation of the article generally is modeling of electrodynamic processes taking place indoors and outdoors, the investigation of possible impact of the EM field on human during exposure and satisfaction of the safety and sanitary standards. Paper summarizes the acquisition of expert knowledge within the main principles and features of the MAS numerical technique in application to 3-D problems and the human exposure due to RF radiation

Using the MAS EM field distribution inside the car model and the room model building with iron- concrete material are simulated. Inside the room built on several frequencies enhance of resonance field is observed. Resonance frequencies depend mainly on the room size, it's dimensions so, every room characterized with its own resonance frequencies. Appearance of the resonance EM fields doesn't depend on the incident field source location. Approximately the same results were observed for

several car cases. Such estimations should be taken into account by motor vehicles manufacturers to reduce influence of electromagnetic radiation on sensitive electronic devices of the machine. The illustrated distributions of fields inside models give an evident picture of EM field distributions occurring in a daily life.

The analysis of the obtained resonant characteristics of models, distributions of currents on the surface can help to estimate behavior of a field in various resonant structures. Knowing this character of distribution and the maximal value of field amplitude in some area of space, it is possible to predict its possible influence on the human situated in this area.

ACKNOWLEDGMENT

We would like to thank Mobile Manufacturers Forum (MMF) and Global System Mobile Association (GSMA) for sponsoring part of this work. Also, we would like to thank George Bit-Babik for constant interests and getting his opinion to these investigations.

REFERENCES

[1] H. Lehmann, P. Fritschi, B. Eicher, Swisscom, Bern, Switzerland: “The variability of the electric field in rooms near mobile phone base stations”. Proceedings of 15th International Zurich Symposium & Technical Exhibition on EMC 2003. February 18-20. pp 161-166. 30F4

[2] R. Zaridze, G. Bit-Babik, K. Tavzarashvili, N. Uzunoglu, D. Economou. "Wave Field Singularity Aspects Large-Size Scatterers and Inverse Problems." IEEE Transactions on Antennas and Propagation, vol. 50, No. 1, January 2002, p. 50-58.

[3] Jungwon Lee, “Protecting the Method of Auxiliary Sources (MAS) Solutions from the Interior Resonance Problem”. IEEE Microwave and Wireless Components Letters, vol.15, no.3, pp 186-188, March 2005.

[4] J. R. Mautz and R.F. Harrington, “A combined-source solution for radiation and scattering from a perfectly conductive body”, IEEE Trans. Antennas Propagat., vol. 27, no. 4, pp 445-454, July 1979.

[5] V.V. Nikolski, Electrodynamics and Wave Propagation, Moscow, “NAUKA”, 1978, 544p.p. Russia.

[6] R. Zaridze, G. Bit-Babik, K. Tavzarashvili, A. Bijamov, D. Kakulia, G. Ghvedashvili "The Method of Auxiliary Sources in Scattering and Diffraction Problems" is presented on 2001 IEEE AP-S International Symposium, Boston, Massachusetts, July 8-13, 2001.